X-Ray Crystallographic, Spectroscopic, and Energy Calculation Studies of the 3-Carbamoyl-1-[3-(indol-3-yl)propyl]pyridinium Ion, a Charge-transfer Interaction Model between Tryptophan and Pyridine Coenzymes †

Toshimasa Ishida,* Sachiko Ibe, and Masatoshi Inoue
Osaka College of Pharmacy, 2-10-65 Kawai, Matsubara-City, Osaka 580, Japan

The title compound was synthesized in order to elucidate the intramolecular stacking geometry between the indole and pyridinium rings, and its crystal structure was determined by *X*-ray analysis. The structure was solved by direct methods and refined by least-squares to a final *R* index of 0.105. In the crystal, the prominent stacking interaction between the indole ring and its nearest neighbouring pyridinium ring, which is favourable for the charge-transfer interaction of both aromatic rings, was observed, although the molecule took a fully extended conformation. This stacking mode, the parallel alignment of both rings, and the spacing near to the normal van der Waals separation distance, was stabilized by Coulombic attraction forces and the interaction between the highest occupied molecular orbital of the indole ring and the lowest unoccupied one of the pyridinium ring. However, the absorption spectra showed the existence of the intramolecularly stacked charge-transfer interaction of both aromatic rings. This stacked conformation was also suggested by fluorescence and ^{1}H n.m.r. spectra. Empirical potential-energy calculations, using the minimization technique, showed the four kinds of intramolecularly stacked conformers to be energetically stable.

Charge-transfer interaction between donor and acceptor molecules possesses certain properties that could be important in biological systems.[2,3] It is well known that the indole derivatives form π–π charge-transfer complexes with pyridine coenzymes such as nicotinamide adenine dinucleotide (NAD^+). These complexes could be characterized by an intense yellow colouration due to a marked increase of absorbance in the 300—500 nm region,[4,5] which is a region far from the absorption maximum of either of the component molecules. Such a spectroscopic property is also observed between various 1-substituted 3-carbamoylpyridinium ions and indole compounds.[5-7] Therefore, the main binding site of tryptophan appears to be the nicotinamide moiety of the pyridine coenzymes, although the interaction with the adenine moiety could not be neglected.[8]

On the other hand, this characteristic charge-transfer formation due to the indole–pyridinium ring association is, as has already been pointed out by Cilento and Tedeschi,[5] a useful probe for detecting the exposed tryptophan residues in proteins, and has been widely used in the study of the stereochemical environments of tryptophyl residues using 1-substituted 3-carbamoylpyridinium derivatives.[9-13]

The elucidation of the mode of the charge-transfer interaction between indole and 1-substituted 3-carbamoylpyridinium rings is therefore important for the following reasons: it may provide insights into the role of the tryptophan residue in pyridine coenzyme–apoenzyme binding, and to a more detailed understanding of how the environment of a tryptophyl residue affects the binding of pyridinium analogues.

X-Ray crystallography, which is a powerful method for such interaction studies at the atomic level, has been applied to three kinds of model crystals, as far as we know: 3-carbamoyl-1-methylpyridinium(1-MNA)·*N*-acetyl-L-tryptophanate,[14] 1-MNA·indole-3-acetate(IAA),[15] and 3-carbamoyl-1-[2-(indol-3-yl)ethyl]pyridinium(IC2P) chloride.[16] The former two complexes, as intermolecular interaction models, have provided information about the strengths of the interaction. The parallel alignment of both aromatic rings and the vertical spacing near to the normal van der Waals separation distance (3.4 Å) are necessary for the π–π charge-transfer interaction. *X*-Ray analysis of the last compound, which was intended to be an intramolecular model for providing information about the geometrical requirements of the interaction,[17] also showed an intermolecular stacking interaction similar to those of the former complexes. The absence of the intramolecular interaction would largely be due to the shortness of the chain connecting the indole and the pyridinium rings and to the effect of the crystal packing forces.

We have carried out *X*-ray crystallographic, spectroscopic, and energy calculation studies of 3-carbamoyl-1-[3-(indol-3-yl)propyl]pyridinium(IC3P); the propylene linkage in IC3P may provide more flexibility between the indole and pyridinium rings and is more suitable for the intramolecular interaction than the ethylene linkage in IC2P.[18]

Experimental

Synthesis of the IC3P Salt.—A crude precipitate of IC3P bromide was synthesized according the literature [19,20] using 3-(indol-3-yl)propionic acid and nicotinamide. The substance, dissolved in appropriate amounts of water, was then applied to a silica gel column (3 cm i.d. × 30 cm, Kieselgel 60, Merck). The column was eluted with 2 000 ml of a mixture of ethyl acetate–methanol–water (5 : 5 : 2, v/v/v). Fractions (20 ml) were collected. The fractions with u.v. maxima of *ca.* 270 nm in aqueous solution were collected, and the solvent was removed by rotary evaporation at a temperature below 30 °C. The product was recrystallized from 30% aqueous ethanol (Found: C, 52.99; H, 5.66; N, 10.93. $C_{17}H_{18}BrN_3O\cdot 3/2H_2O$ requires C, 52.72; H, 5.47; N, 10.85%). The IC3P bromide was then converted into its sulphate for *X*-ray analysis (to give more suitable crystals) or into the chloride salt for the spectroscopic studies using Amberlite IRA-401 anion-exchange resin.

Crystal Structure Determination.—Yellow crystals of IC3P hemisulphate were obtained from aqueous solution by slow evaporation at room temperature. This colour implies

† This work is Part XI [1] of 'Structural Studies of the Interaction between Indole Derivatives and Biologically Important Aromatic Compounds.'

the formation of a charge-transfer interaction. A crystal with dimensions of *ca.* 0.2 × 0.1 × 0.3 mm³ was used for *X*-ray analysis. Preliminary *X*-ray photographs showed the crystal to be triclinic with space group $P1$ or $P\bar{1}$; its space group was finally determined to be centrosymmetric $P\bar{1}$ from the statistical distribution of normalized structure factors.[21] Crystal data are as follows: $C_{17}H_{18}N_3O^+ \cdot 1/2SO_4^{2-} \cdot 7/2H_2O$, $M = 391.43$, $a = 9.692(5)$, $b = 15.320(6)$, $c = 7.117(4)$ Å, $\alpha = 92.93(5)$, $\beta = 117.03(5)$, $\gamma = 93.06(5)°$, $U = 937(1)$ Å³, $D_m = 1.386(2)$ g cm⁻³, $Z = 2$, $D_c = 1.388$ g cm⁻³, μ(Cu-K_α) = 13.8 cm⁻¹, $F(000)$ 416. Cell parameters were determined from 25 reflections having strong reflection intensities with $50° < 2\theta < 60°$ by using a Rigaku automatic four-circle diffractometer with graphite-monochromated Cu-K_α radiation, and were refined by the least-squares method. The crystal density was measured by the flotation method in a benzene–carbon tetrachloride mixture.

Three-dimensional intensities of less than $2\theta = 130°$ were collected by the same diffractometer employing the ω–2θ scan technique with a scan speed of 3° min⁻¹. The measured 3 198 independent intensities were corrected for Lorentz and polarization factors, but not for absorption effects because of the small size of crystal used. Four standard reflections, measured at every 100 reflection intervals, showed no structural deterioration during the data collection.

The structure was solved by the direct method with a MULTAN 78 program: [22] an *E*-map calculated using a phase set of 240 reflections ($E > 1.77$) with the highest combined figure of merit revealed a sulphur atom and some of the non-hydrogen atoms of the IC3P molecule. The remaining non-hydrogen atoms were revealed by subsequent Fourier synthesis. The structure was refined by a block-diagonal least-squares method with anisotropic temperature factors. All the hydrogen atoms, except for those of the water, were positioned by a difference Fourier synthesis, and were included in the subsequent refinements with isotropic temperature factors. The minimized function was $\Sigma w(|F_o| - |F_c|)^2$; in the final refinement, a value of 2.689 01 for weight (w) was used for $F_o = 0.0$, and $w = 1.0/[\sigma^2(F_o) - 0.008\ 18|F_o| + 0.010\ 70|F_o|^2]$ for $F_o > 0.0$. The final R value was reduced to 0.105. Final atomic co-ordinates for the non-hydrogen atoms are listed in Table 1. Lists of structure factors, anisotropic thermal parameters of the non-hydrogen atoms, atomic co-ordinates, and isotropic temperature factors of hydrogen atoms, and possible hydrogen-bond distances have been deposited as Supplementary Publication No. 23781 (16 pp.).* The program used for refinements was the UNICS program.[23] Scattering factors used were those cited in the literature.[24]

Molecular Orbital Calculations.—The permanent dipole moments, the atomic charges, and the energies and their atomic orbital coefficients of the HOMO (highest occupied molecular orbital) or LUMO (lowest unoccupied molecular orbital) for 3-methylindole and 3-carbamoyl-1-methylpyridinium were carried out by the CNDO/2 (complete neglect of differential overlap) method.[25]

Spectroscopic Studies.—U.v. and visible absorption spectra were measured on a Hitachi 624 spectrophotometer with dual compartment cells (10 mm). The relative quantum efficiency of fluorescence was determined on a Hitachi-650-40 spectrofluorimeter using a xenon lamp. The emission spectra were measured by excitation at 295 nm. The absorption and fluorescence spectra were measured three times in a 0.025M-phosphate buffer (pH = 6.8), and were averaged.

^{1}H N.m.r. spectra were recorded with a Varian XL-200 (200 MHz, FT-mode) spectrometer equipped with a variable-temperature accessory. Chemical shifts were measured against DSS (sodium 2,2-dimethyl-2-silapentane-5-sulphonate) as an standard internal.

Conformation Energy Calculations.—The energies for various IC3P conformations were calculated by the empirical PPF (partitioned potential-energy function) method (programmed by Dr. S. Fujii, Pharmaceutical Sciences, Osaka University). The functions included in the calculations were non-bonded (E_{nb}), electrostatic (E_{el}), and torsional (E_t) energies. These quantities (in kilocalories per mol) can be obtained by computing equations (1)—(3) where R_{IJ} is the observed distance

$$E_{nb} = \sum_{I>J}\sum (-A_{IJ}R_{IJ}^{-6} + B_{IJ}R_{IJ}^{-12}) \quad (1)$$

$$E_{el} = \sum_{I>J}\sum 332.0 \times Q_I \times Q_J \times R_{IJ}^{-1} \times \varepsilon^{-1} \quad (2)$$

$$E_t = \sum_{k=1}^{N} 0.5 \times V_k \times (1.0 + \cos X\theta_k) \quad (3)$$

Table 1. Positional parameters (× 10⁴) of non-hydrogen atoms

Atom [a]	*x*	*y*	*z*
IC3P			
N(1)I	11 369(5)	6 830(2)	10 226(7)
C(2)I	10 053(5)	7 231(3)	9 832(7)
C(3)I	10 317(4)	8 114(3)	9 939(6)
C(4)I	12 899(5)	9 035(3)	10 785(6)
C(5)I	14 437(5)	8 977(3)	11 325(8)
C(6)I	15 040(5)	8 137(4)	11 470(7)
C(7)I	14 080(5)	7 377(3)	11 125(7)
C(8)I	12 544(5)	7 456(3)	10 610(6)
C(9)I	11 932(4)	8 272(3)	10 430(6)
C(10)	9 229(4)	8 816(3)	9 655(7)
C(11)	7 565(4)	8 464(3)	9 082(6)
C(12)	6 616(5)	8 238(3)	6 766(7)
N(1)N	4 995(4)	7 936(2)	6 278(5)
C(2)N	3 971(4)	8 530(3)	5 974(6)
C(3)N	2 473(4)	8 279(3)	5 591(6)
C(4)N	2 031(5)	7 384(3)	5 511(7)
C(5)N	3 132(6)	6 788(3)	5 804(9)
C(6)N	4 608(5)	7 084(3)	6 171(8)
C(7)N	1 411(4)	8 992(3)	5 302(6)
N(8)N	−25(4)	8 774(2)	4 935(6)
O(9)N	1 933(4)	9 756(2)	5 384(7)
Sulphate ion			
S [b]	3 273(2)	4 734(1)	9 974(4)
O(1) [b]	3 080(6)	3 856(3)	9 849(7)
O(2) [c]	4 359(19)	4 991(12)	9 036(26)
O(3) [c]	3 905(18)	5 067(9)	12 004(22)
O(4) [c]	1 784(20)	5 059(10)	8 542(35)
O(5) [c]	2 556(26)	5 104(14)	8 154(37)
O(6) [c]	4 915(20)	5 069(13)	11 326(35)
O(7) [c]	2 458(24)	5 123(11)	11 257(35)
Waters of crystallization			
O(1)W	1 657(5)	2 981(3)	5 893(7)
O(2)W	6 877(9)	5 602(5)	15 115(10)
O(3)W [b]	232(43)	4 709(17)	14 216(33)
O(4)W [b]	506(21)	4 931(11)	8 755(31)
O(5)W [b]	985(19)	5 019(9)	11 463(27)

[a] The suffixes I, N, and W in the atom designations refer to indole and pyridinium rings, and water molecules, respectively. [b] Occupancy of atom is 0.50. [c] Occupancy of atom is 0.25.

* For details for the Supplementary Publications Scheme see Instructions for Authors (1984), *J. Chem. Soc., Perkin Trans. 2*, 1984, Issue 1.

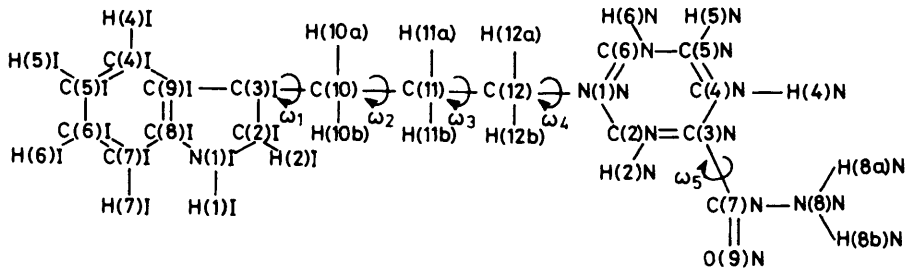

Figure 1. Atomic numberings and torsional notations used for the IC3P molecule

(Å) between atoms i and j, and A_{ij} and B_{ij} are the coefficients in the Lennard-Jones '6–12' potential function; Q_i is the net charge on atom i, and ε is the dielectric constant (and equals 4.0); V_k is the barrier potential for the internal rotation about the kth torsion angle (θ_k), X is the periodicity of the barrier, and N is the number of variable torsion angles. The notation of variable torsion angles in the IC3P molecule is illustrated in Figure 1. The values of A_{ij} and B_{ij} were taken from the literature;[26-29] Q_i was calculated by the CNDO/2 method by using the co-ordinates of IC3P; V_k was taken as 2.5 kcal mol^{-1} for a C–C single bond,[27] and 0 kcal mol^{-1} for a C–N bond;[26,27] X was taken as 3 for a C–C bond and as 6 for a C–N bond, respectively. For energy minimization, each torsion angle as a variable parameter was optimized by the Powell algorithm.[30] Minimization was carried out by parabola approximation with 4° intervals, and no angle was permitted to vary by more than 12° at each step.

All numerical calculations were carried out on an ACOS-900 computer at the Crystallographic Research Center, Institute for Protein Research, Osaka University.

Results and Discussion

Molecular Structure.—Bond lengths and angles for the non-hydrogen atoms are presented in Figure 2; the Figure also shows the IC3P molecular conformation observed in the crystal, projected onto the indole ring moiety.

Standard deviation ranges from 0.006 to 0.008 Å for bond lengths and 0.4 to 0.5° for bond angles; the bond lengths involving hydrogen atoms range from 0.73[N(1)I–H(1)I] to Å[1.12C(10)–H(10a)]; the bond angles found are acceptable.

Both the listed bond distances and angles appear normal within their estimated standard errors, compared with related indole and 3-carbamoylpyridinium compounds.[14-16,31-35] Three oxygen atoms of the sulphate ion are in a state of disorder around the S–O(1) axis, and the O(2)—O(7) atoms have occupancies of 0.25. Therefore, the listed values are somewhat uncertain, but the values are all within the accepted ranges.[36]

The least-squares planes and the deviations of the respective atoms from them were calculated for the indole and pyridinium rings. Both the aromatic rings are almost planar with a maximum deviation of 0.022(6) Å [C(5)I] for the indole ring and −0.011(7) Å [C(6)N] for the pyridinium ring; the root mean square deviation is 0.01 Å for the former ring and 0.006 Å for the latter.

The indole ring is almost parallel to the pyridinium ring with a dihedral angle of 3.2(2)°; this is in strict contrast to the IC2P molecule.[16] in which both the rings are almost perpendicular to each other (dihedral angle = 87°).

The selected torsion angles are listed in Table 2. The IC3P molecule takes a fully extended conformation; the *trans* orientation of the torsion angle ω_3 gives both the aromatic

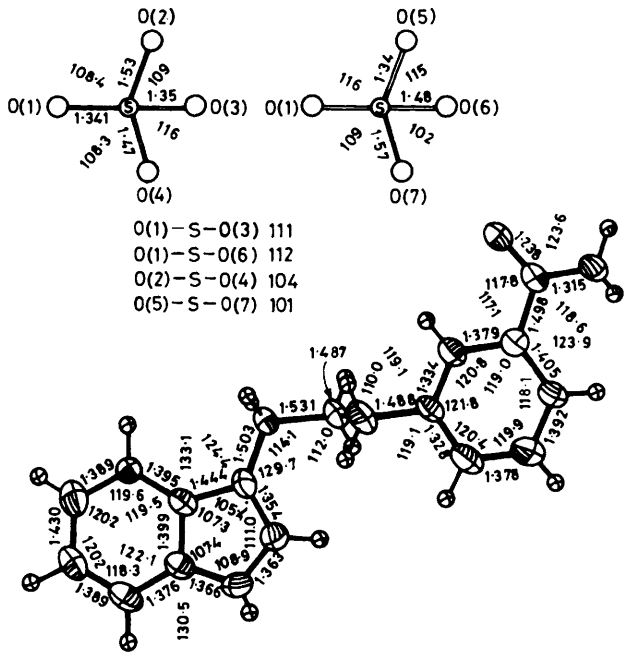

Figure 2. Bond lengths and angles between non-hydrogen atoms. Estimated standard deviations for sulphate ion range from 0.006 to 0.03 Å for the bond lengths and 0.8 to 1.2° for angles, respectively

rings an extended alignment. Such an extended conformation has also been observed in the IC2P molecule.

The plane of the carbamoyl group makes an angle of 178.6(5)° with the plane of the pyridinium ring, and the Q(9)N atom takes a *cis* orientation to the C(2)N atom with a torsion angle, ω_5, of 1.4(6)°. Since this ω_5 value of *ca.* 0° is frequently observed in many related compounds, the almost coplanar alignment of these two groups would therefore be a favourable conformation for the 3-carbamoylpyridinium ring, although the molecular orbital calculations for oxidized nicotinamide predicts the conformation that has ω_5 of *ca.* ±30° to be the most energetically stable form.[37]

Molecular Packing and Hydrogen Bonding.—The partial molecular packing viewed along the c-axis is shown in Figure 3; of the waters of crystallization, indicated by the filled-in circles, O(3)W—O(5)W are in disorder and have occupancies of 0.5. A stereoscopic view is shown in Figure 4.

The indole moiety of the IC3P molecule is predominantly stacked with the pyridinium moiety of the neighbouring molecule, consequently making the molecular packing along the a-axis stable. All available hydrogen atoms participated in

Table 2. Selected torsion angles (°) of IC3P

C(2)I–C(3)I–C(10)–C(11), ω_1	−2.4(7)
C(9)I–C(3)I–C(10)–C(11)	178.4(4)
C(3)I–C(10)–C(11)–C(12), ω_2	−85.0(5)
C(10)–C(11)–C(12)–N(1)N, ω_3	−177.6(4)
C(11)–C(12)–N(1)N–C(2)N, ω_4	86.1(5)
C(11)–C(12)–N(1)N–C(6)N	−93.4(5)
C(2)N–C(3)N–C(7)N–N(8)N	−180.0(4)
C(2)N–C(3)N–C(7)N–O(9)N, ω_5	1.4(6)
C(4)N–C(3)N–C(7)N–N(8)N	−0.6(7)
C(4)N–C(3)N–C(7)N–O(9)N	−179.2(5)

the hydrogen-bond formations with reasonable distances. The carbamoyl group was linked with the centrosymmetrically related one by two hydrogen-bond formations of N(8)–H(8) ··· O(9) [2.943(6) Å], which is a frequently observed bonding mode for this group.[38] The N(8) atom is further hydrogen bonded to the O(1)W [2.935(7) Å]. However, the N(1) atom of the indole ring was hydrogen bonded to the disordered oxygen atoms of the sulphate ion and water molecules, with reasonable distances (2.88—3.03 Å). Many possible hydrogen bonds were further formed between the oxygen atoms of the sulphate ion and water molecule and between the neighbouring sulphate ions or water molecules; the details were deposited in the Supplementary Publication. These hydrogen-bond formations stabilize the molecular packing to the *b*- and *c*-axis.

Stacking Interaction between Indole and Pyridinium Rings in the Crystalline State.—Figure 5 illustrates the stacking modes between the indole and pyridinium rings observed in this crystal structure with the two up-and-down stacked pyridinium rings being viewed perpendicular or parallel to the central indole ring. The indole ring is almost parallel and takes a dihedral angle of 3.2(2)° to either pyridinium ring. Seven short contacts of less than 3.5 Å are observed in the upper pair and two in the lower pair (see also Table 3). The average interplanar spacing in the area of overlap is 3.407 Å for the upper pair and 3.480 Å for the lower one. While the spacing of the latter is far from the normal van der Waals separation distance (3.4 Å), that of the former case is very near to 3.4 Å, implying that this stacking formation is largely stabilized by van der Waals short contacts between both the aromatic rings. Although there is no evidence concerning the partial charge-transfer interaction between the indole ring to the unoccupied molecular orbital of the pyridinium ring in their ground states, it appears to be a favourable stacking mode for the charge-transfer interaction in the energy transitions from their ground states to the excited ones, because of the colour change from the colourless aromatic ring compounds to the yellowish IC3P crystals and because of the noticeable appearance of a charge-transfer band in the absorption spectrum (see below).

Some stacking parameters and orientations concerning indole–pyridinium ring interactions have already been summarized.[15] The relative orientation of the pyridinium ring with respect to the indole ring in the IC3P crystal is similar to that of *N*-acetyl-L-tryptophan : 1-MNA (1 : 1) complex [14] with the dipole–dipole interaction between the indole and pyridinium rings almost uncoupled. This stacking mode of IC3P is in strict contrast with that of the related IC2P molecule,[16] in which the ring orientation is largely specified by the dipole–dipole interaction between both of the aromatic rings.

It seems likely that the mutual orientation of the stacked rings in IC3P is stabilized by Coulombic attractions as in the *N*-acetyl-L-tryptophan : 1-MNA and IAA : 1-MNA [15] com-

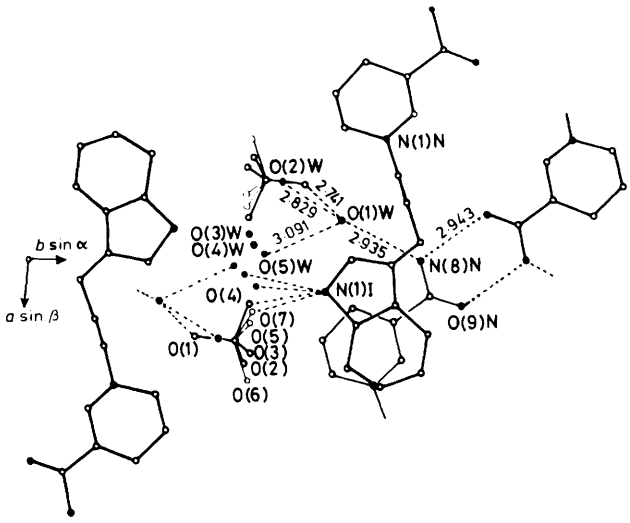

Figure 3. Molecular packing viewed along the *c*-axis. Waters of crystallization are represented by filled-in circles; dotted lines represent possible hydrogen bonds. The hydrogen bonds between sulphate ion and water molecule and between neighbouring sulphate ions or water molecules were omitted for the sake of clarity

plexes, because many of short contact pairs occur between two atoms capable of forming an electron-rich and electron-deficient pair: −0.036e—0.032e for C(6)I–C(12), −0.036e—0.081e for C(6)I–N(1)N, −0.053e—0.081e for C(7)I–N(1)N, and −0.053e—0.142e for C(7)I–C(6)N (these atomic charges were calculated by the CNDO/2 method using the co-ordinates of the 3-methylindole and 1-MNA molecules, respectively). Further, the interaction between the HOMO of the indole ring and the LUMO of the pyridinium ring would also, in parts, participate in specifying the ring orientation, because as is shown in Table 3, nine out of 13 short contact pairs of less than 3.6 Å have the same signs as each other in the respective atomic coefficients of the HOMO (indole ring) and in the LUMO (pyridinium ring), implying that their respective atomic orbitals interact with each other in the electron transitions.

Interactions between the Indole and Pyridinium Rings of the IC3P Molecule in Aqueous Solution.—Contrary to our objective of elucidating a possible intramolecular stacking geometry, the IC3P molecule in its crystal took a fully extended form, probably due to the crystal packing requirements. However, the u.v. and visible absorption spectra clearly indicated the intramolecular stacking interaction to exist predominantly in aqueous solution. Absorption spectra are shown in Figure 6, where the concentration of sample used (1.0×10^{-4} M) should reflect the spectral properties caused by the intramolecular interaction rather than the intermolecular one. A difference spectrum of IC3P chloride against 1-MNA chloride plus 3-methylindole shows the hypochromic effect due to the stacking interaction between both of the aromatic rings in the range 243—293 nm. A charge-transfer band was observed in the region of from 300 to 480 nm ($\lambda_{max.}$ = 320 nm, $\varepsilon_{320\ nm}$ = 1 387 dm^3 mol^{-1} cm^{-1}). Such a charge-transfer band has also been observed in many indole–pyridinium-containing systems.[39]

Further, the fluorescence emission spectrum of the IC3P chloride, compared with that of 3-methylindole, indicated the almost complete quenching of the indole fluorescence (its quantum yield is 0.005 at 370 nm, with reference to 3-methyl-

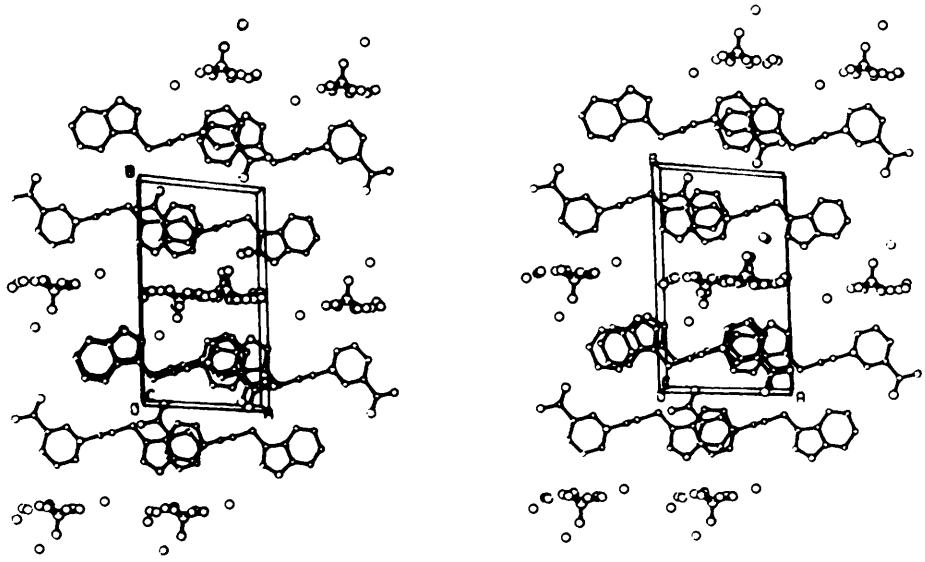

Figure 4. Stereoscopic view of IC3P crystal viewed along the *c*-axis

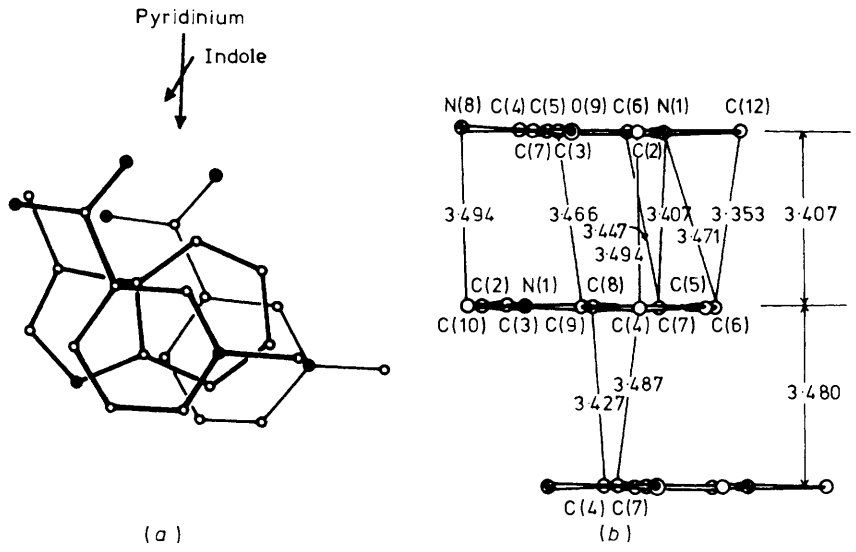

Figure 5. Stacking mode of nearest-neighbour indole–pyridinium rings, projected perpendicular (*a*) or parallel (*b*) to the indole ring. The relative magnitudes and directions of the calculated permanent dipole moments for the ground states of 3-methylindole (1.85 D) and 1-MNA cation (3.37 D) are shown above structure (*a*). These values were calculated by the CNDO/2 method

indole). This also implies the prominent existence of the intramolecularly stacked form in its excited state.

Such stacking interaction was also observed from the temperature dependence of the aromatic protons for the chemical shifts of IC3P chloride in [$^2H_2$]O solution (0.001M). The results are given in Table 4; the peak assignments of aromatic protons were done by reference to related literature [40] and spin multiplicities, but the assignments for the H(4) and H(6) protons of the pyridinium ring is tentative. Respective aromatic protons shift upfield, in proportion to the decrease in the measured temperature. This change of chemical shifts could be interpretable as the ring current effect between both the aromatic rings, suggesting the existence of ring-stacking interactions.

Conformational Analysis of the IC3P Molecule by Empirical Energy Calculations.—Although crystal analysis showed no intramolecular stacking interaction, its existence in the dilute aqueous solution was obvious from the spectroscopic studies. Therefore, we carried out the conformational analysis of the IC3P molecule using the empirical PPF method in order to obtain the energetically stable conformation with intramolecular stacking.

The starting angles for the refinements of five kinds of variable torsion angles (see Figure 1) were selected as the most reasonable values from the various investigations as follows: ω_1 and $\omega_4 = \pm 30°, \pm 90°$, and $\pm 150°$, ω_2 and $\omega_3 = \pm 60°$ and 180°, and $\omega_5 = 0°$. Out of 324 different sets, 10 energetically stable conformations are listed in Table 5, together with their starting sets and final energies. In this Table the energy for the conformation observed in this crystal structure is also listed.

It is of interest to note that sets with either 60° or −60° as the starting angle for ω_2 and ω_3 introduce the energetically stable folded conformation with the stacking of both arom-

Table 3. Orbital interaction in the atoms between the HOMO of the indole ring and the LUMO of the pyridinium ring in the upper stacked atomic pairs (less than 3.6 Å) [a]

Atom (indole)	Atom (pyridinium)	Distance	HOMO	LUMO	Orbital interaction [b]
N(1)	C(4)	3.564	0.4293	−0.5593	−
N(1)	C(5)	3.544	0.4293	0.1063	+
C(2)	C(4)	3.588	−0.4098	−0.5593	+
C(3)	C(3)	3.579	−0.4941	0.1833	−
C(4)	C(2)	3.494	0.3297	0.3572	+
C(6)	C(12)	3.353	−0.3091	−0.0309	+
C(6)	N(1)	3.471	−0.3091	−0.5133	+
C(7)	N(1)	3.407	−0.2855	−0.5133	+
C(7)	C(6)	3.447	−0.2855	0.4644	−
C(9)	C(2)	3.507	0.0914	0.3572	+
C(9)	C(3)	3.466	0.0914	0.1833	+
C(10)	N(8)	3.494	0.1213	−0.0398	−
C(10)	C(7)	3.578	0.1213	0.0635	+

[a] These values were calculated by the CNDO/2 method using the co-ordinates of 3-methylindole and 1-MNA molecules. [b] Orbital coupling designated by + or −, respectively.

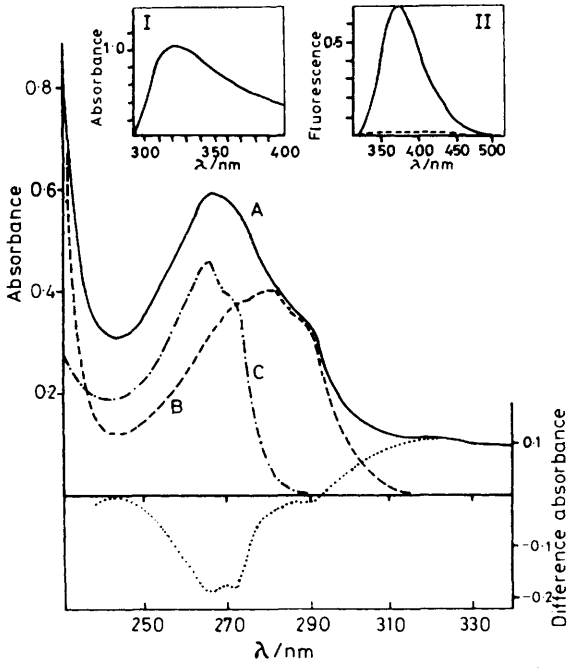

Figure 6. Ultraviolet absorption spectra of IC3P chloride (A), 3-methylindole (B), and 1-MNA chloride (C), and their difference spectrum [IC3P chloride − (1-MNA chloride + 3-methylindole)] (· · · ·) in 0.025M phosphate buffer (pH 6.8) containing samples at concentrations of 1.0×10^{-4}M at 25 °C

Insert I: Charge-transfer band ranging from 300 to 410 nm. Absorbance was measured at 25 °C using 7.5×10^{-4}M-IC3P chloride. Insert II: Fluorescence emission spectra of 3-methylindole (——) and IC3P chloride (· · · ·) measured at 295 nm excitation using 1.0×10^{-4}M concentrations (25 °C)

atic rings, while the conformations having 180° as the starting angle of either ω_2 or ω_3 unequivocally converged to the extended and metastable forms having energy values of −10—12 kcal mol^{-1}. The observed conformation in the crystal structure also belongs to this category.

In the energetically stable intramolecular stacking conformation, four kinds of modes were observed; these are represented by the letters A, A′, B, and B′ in Table 5. The most stable conformations in respective stacking modes are illustrated in

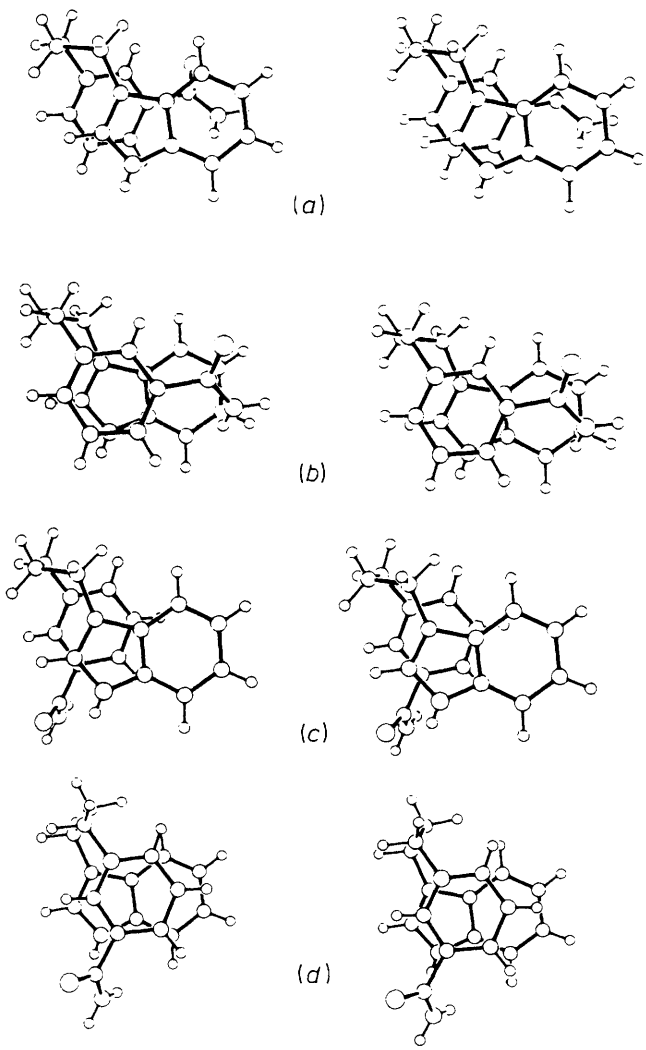

Figure 7. Calculated models of IC3P molecule having the energetically stable conformation. (*a*) Set No. 1 of Table 5, conformer A; (*b*) set No. 2, conformer A′; (*c*) set No. 5, conformer B; (*d*) set No. 4, conformer B′

Table 4. Temperature dependence of chemical shifts of aromatic protons (p.p.m.), referred to DSS as an internal standard. Error is ±0.002 p.p.m.

Temp. (°C)	Pyridinium				Indole				
	H(2)	H(4)	H(5)	H(6)	H(2)	H(4)	H(5)	H(6)	H(7)
10	8.683	8.523	7.391	8.152	7.008	7.330	6.900	7.062	7.225
30	8.729	8.554	7.492	8.241	7.041	7.376	6.940	7.098	7.274
50	8.770	8.586	7.583	8.322	7.066	7.414	6.974	7.127	7.300

Table 5. Starting and final torsion angles (°) and their energies

No.	Starting angle					Final angle					Energy kcal mol^{-1}	Conformer
	ω_1	ω_2	ω_3	ω_4	ω_5	ω_1	ω_2	ω_3	ω_4	ω_5		
1	−30	−60	60	−90	0	−37	−76	54	−101	−52	−20.4	A
2	30	60	−60	90	0	34	78	−54	101	42	−20.1	A′
3	30	−60	60	−90	0	−31	−79	49	−98	−54	−19.7	A
4	90	−60	60	−150	0	128	−62	72	−112	−62	−19.3	B′
5	−30	−60	60	90	0	−41	−78	50	75	−60	−19.2	B
6	−30	−60	60	−150	0	−41	−66	75	−107	−58	−19.1	A
7	30	−60	60	90	0	−40	−80	48	73	−63	−19.0	B
8	−30	60	−60	90	0	26	84	−59	97	67	−19.0	A′
9	30	60	−60	−90	0	43	80	−45	−72	−59	−18.8	B′
10	150	−60	60	−90	0	129	−66	66	−111	62	−18.5	B′
Cryst.	−2	−85	−178	86	1						−10.5	

Figure 7, in which the molecules are projected onto the indole ring. A significant difference between conformers A and A′ or between B and B′ is the stacking side between both aromatic rings: the pyridinium ring is stacked with the upper side of the indole ring or the lower one. On the other hand, the conformers A and B, in addition to A′ and B′, could almost be related to each other by 180° rotation around the C(12)–N(1)N bond. These results mean that the pyridinium ring could be well stacked with the upper side and with the lower side of the indole ring; in other words, the pyridinium ring could interact with both sides of the indole ring with equal stacking forces.

Comparing the intermolecular stacking modes elucidated by *X*-ray analyses,[14–16] there is no resemblance with the intramolecular stacking modes, although one of two kinds of modes that exist in the IAA : 1-MNA complex could be, in some aspects, similar to conformer A. This may imply that the stable stacking modes are different in the inter- and intramolecular interactions.

It is worthwhile noting that conformers A and A′ are largely stabilized by Coulombic attraction forces between both aromatic rings, while conformers B and B′ are stabilized by the strong dipole–dipole coupling, judging from the CNDO/2 results.

References

1 Part X. T. Ishida, M. Shibata, K. Fujii, and M. Inoue, *Biochemistry*, 1983, **22**, 3571.
2 R. S. Mulliken, *J. Am. Chem. Soc.*, 1952, **74**, 811.
3 E. M. Kosower, *J. Am. Chem. Soc.*, 1956, **78**, 3497.
4 I. Isenberg and A. Szent-Györgyi, *Proc. Natl. Acad. Sci. USA*, 1959, **45**, 1229.
5 G. Cilento and P. Tedeschi, *J. Biol. Chem.*, 1961, **236**, 907.
6 S. G. A. Alivasatos, F. Unger, A. Jibril, and G. A. Mourkides, *Biochim. Biophys. Acta*, 1961, **51**, 361.
7 C. Cilento and P. Guisti, *J. Am. Chem. Soc.*, 1959, **81**, 3801.
8 K. J. Neurohr and H. H. Mantsch, *Can. J. Chem.*, 1979, **57**, 2297.
9 K. Ikeda and K. Hamaguchi, *J. Biochem. (Tokyo)*, 1973, **74**, 221.
10 K. Ikeda and K. Hamaguchi, *J. Biochem. (Tokyo)*, 1975, **77**, 1.
11 L. M. Hinman, C. R. Coan, and D. A. Deranleau, *Biochemistry*, 1976, **15**, 2212.
12 F. M. Robbins and L. G. Holmes, *J. Biol. Chem.*, 1972, **247**, 3062.
13 D. A. Deranleau, L. M. Hinman, and C. R. Coan, *J. Mol. Biol.*, 1975, **94**, 567.
14 R. P. Ash, J. R. Herriott, and D. A. Deranleau, *J. Am. Chem. Soc.*, 1977, **99**, 4471.
15 T. Ishida, K. Tomita, and M. Inoue, *Arch. Biochem. Biophys.*, 1980, **200**, 492.
16 J. R. Herriott, A. Camerman, and D. A. Deranleau, *J. Am. Chem. Soc.*, 1974, **96**, 1585.
17 S. Shifrin, *Biochim. Biophys. Acta*, 1964, **81**, 205.
18 F. Hirayama, *J. Chem. Phys.*, 1965, **42**, 3163.
19 K. Mutai, B. A. Gruber, and N. J. Leonard, *J. Am. Chem. Soc.*, 1975, **97**, 4095.
20 T. G. Scott, R. D. Spencer, N. J. Leonard, and G. Weber, *J. Am. Chem. Soc.*, 1970, **92**, 687.
21 I. L. Karle, K. S. Dragonette, and S. A. Brenner, *Acta Crystallogr.*, 1965, **19**, 713.
22 P. Main, S. E. Hull, L. Lessinger, G. Germain, J. P. Declercq, and M. M. Woolfson, MULTAN 78, A System of Computer Programs for the Automatic Solution of Crystal Structures from X-Ray Diffraction Data, Universities of York and Louvain, Belgium, 1978.
23 T. Ashida, UNICS-Osaka, The Computer Center, Osaka University, Osaka, Japan, 1979.
24 D. T. Cromer and J. T. Waber, in 'International Tables for X-Ray Crystallography,' eds. J. A. Ibers and W. C. Hamilton, Kynoch Press, Birmingham, 1974, vol. 4, p. 71.
25 J. A. Pople and G. A. Segal, *J. Chem. Phys.*, 1966, **44**, 3289.
26 F. A. Momany, R. F. McGuire, A. W. Burgess, and H. A. Scheraga, *J. Phys. Chem.*, 1975, **79**, 2361.
27 A. V. Lakshminarayanan and V. Sasisekharan, *Biopolymers*, 1969, **8**, 475.
28 V. Renugopalakrishnan, A. V. Lakshminarayanan, and V. Sasisekharan, *Biopolymers*, 1971, **10**, 1159.
29 N. Yathindra and M. Sundaralingam, *Biopolymers*, 1973, **12**, 297.
30 M. J. D. Powell, *Comput. J.*, 1964, **7**, 155.
31 T. Ishida, Ph.D. Thesis, Osaka University, 1979, p. 125.

32 A. Camerman, L. H. Jensen, and A. T. Balaban, *Acta Crystallogr., Sect. B*, 1969, **25**, 2623.
33 P. L. Johnson, C. A. Maier, and I. C. Paul, *J. Am. Chem. Soc.*, 1973, **95**, 5370.
34 P. L. Johnson, J. K. Frank, and I. C. Paul, *J. Am. Chem. Soc.*, 1973, **95**, 5377.
35 D. Voet, *J. Am. Chem. Soc.*, 1973, **95**, 3763.
36 H. Ondik and D. Smith, in 'International Tables for X-Ray Crystallography,' eds. C. H. Macgillavry, G. D. Rieck, and K. Lonsdale, Kynoch Press, Birmingham, 1968, vol. 3, p. 272.
37 J. L. Coubeils, B. Pullman, and Ph. Courrière, *Biochem. Biophys. Res. Commun.*, 1971, **44**, 1131.
38 L. Leiserowitz and G. M. J. Schmidt, *J. Chem. Soc. A*, 1969, 2372.
39 D. A. Deranleau and R. Schwyzer, *Biochemistry*, 1970, **9**, 126.
40 S. P. Hiremath and R. S. Hosmane, *Adv. Heterocycl. Chem.*, 1973, **15**, 277.

Received 14*th March* 1983; *Paper* 3/391